Nuclear Instruments and Methods in Physics Research A 692 (2012) 88–92

Contents lists available at SciVerse ScienceDirect

Nuclear Instruments and Methods in Physics Research A

journal homepage: www.elsevier.com/locate/nima

Large scale anisotropy studies with the Pierre Auger Observatory

R. Bonino [a,b,*]

[a] Istituto Nazionale di Astrofisica – IFSI, c.so Fiume 4, 10133 Torino, Italy
[b] INFN sezione di Torino, v. P. Giuria 1, 10125 Torino, Italy

For the Pierre Auger Collaboration[1]

ARTICLE INFO

Available online 17 January 2012

Keywords:
Ultra-high energy cosmic rays
Large scale anisotropies
Pierre Auger Observatory

ABSTRACT

Completed at the end of 2008, the Pierre Auger Observatory has been continuously operating for more than seven years. We present here the analysis techniques and the results about the search for large scale anisotropies in the sky distribution of cosmic rays, reporting both the phase and the amplitude measurements of the first harmonic modulation in right ascension in different energy ranges above 2.5×10^{17} eV. Thanks to the collected statistics, a sensitivity of 1% at EeV energies can be reached. No significant anisotropies have been observed, upper limits on the amplitudes have been derived and are here compared with the results of previous experiments and with some theoretical expectations.

1. Introduction

The measurement of the anisotropy in the arrival directions of cosmic rays (CRs) is a complementary tool, with respect to the energy spectrum and the mass composition, to investigate the nature and the origin of these particles.

In particular, the transition from a galactic to an extragalactic origin should induce a significant change in the CR large scale angular distribution, leading from a large to an almost null amplitude of the CR anisotropy. Such transition is expected in the energy range ($10^{17}-10^{19}$ eV) but it has never been conclusively detected by any experiment. Different models have been proposed to describe it, the most widely known are:

- *The ankle model* [1]: the spectral feature known as "ankle", a sharp change of slope around 3×10^{18} eV (see e.g. Refs. [2,3]), is here explained as the signature of the transition from a heavy galactic component to a predominantly light extragalactic component. Additional mechanisms able to accelerate cosmic rays in galactic sources up to such high energies must however be introduced.
- *The dip model* [4]: another remarkable but less evident change of slope is expected in the energy interval 1×10^{18}–4×10^{19} eV. Such spectral feature called "dip" should be attributed, according to this model, to the electron-positron production by extragalactic UHE protons impacting on the microwave background (CMB). The transition is therefore expected at energies lower than the dip, around the so-called "second knee" ($\sim 1-5 \times 10^{17}$ eV).
- *The mixed composition model* [5]: it assumes that the extragalactic cosmic ray source composition is mixed and similar to the galactic one. The transition region covers energies up to the ankle, while the galactic component extends up to more than 10^{18} eV. The composition could be dominated by protons below 10^{18} eV, unlike in the ankle model.

Different models therefore place the transition at different energies. A measure of the anisotropy at EeV energies or the eventual bounds on it are thus relevant to constrain different models for the CR origin. Due to the limited statistics, current experimental results do not allow any firm conclusion to be drawn. The AGASA experiment, using 11 years of data, reported a 4% dipolar amplitude, significant at the level of 4 s.d., oriented near the Galactic Center at $E \approx 0.8-2 \times 10^{18}$ eV [6]. The Fly's Eye experiment suggested the possibility of an enhancement in the galactic plane at 10^{18} eV [7], and the SUGAR experiment claimed a localized excess from a direction near the Galactic Center [8]. However the Pierre Auger Observatory has not confirmed any of the observed excesses [9]. In the next few years the present experiments, in particular the Pierre Auger Observatory itself, will collect enough statistics to provide additional information to probe this energy range.

We present here the results of the harmonic analysis performed on the events recorded by the Pierre Auger Observatory from 1 January 2004 to 31 December 2009. The total number of events with energy greater than 1 EeV amounts to $\sim 3 \times 10^5$ and

* Correspondence address: Istituto Nazionale di Astrofisica – IFSI, c.so Fiume 4, 10133 Torino, Italy.
E-mail address: rbonino@to.infn.it
[1] Observatorio Pierre Auger, Av. San Martin Norte 304, 5613 Malargüe, Argentina (full author list: http://www.auger.org/archive/authors_2010_11.html).

0168-9002/$ - see front matter © 2012 Elsevier B.V. All rights reserved.
doi:10.1016/j.nima.2011.12.076

already allows one to be sensitive to intrinsic anisotropies with amplitudes down to 1% level.

2. Data set

The southern site of the Pierre Auger Observatory [10] is located in Malargüe, Argentina, at latitude 35.2°S, longitude 69.5°W and mean altitude 1400 m above sea level. It combines two complementary techniques: a *Surface Detector* array of 1660 stations, spread over an area of about 3000 km^2, and a *Fluorescence Detector* of 27 telescopes arranged in four sites overlooking the SD area. The SD detects the Cherenkov light emitted by particles crossing the stations; it measures the lateral distribution and the arrival direction of the shower with a duty cycle of almost 100%. The FD, on the other hand, detects the fluorescence light emitted by nitrogen molecules excited by the cascade and measures the longitudinal profile of the shower during its development in the atmosphere, making almost a calorimetric measure of its energy.

In the analysis reported here we considered only events recorded by the Surface Detector with reconstructed zenith angles smaller than 60° and satisfying a fiducial cut requiring that the six neighboring detectors in the hexagon surrounding the station with the highest signal were active when the event was recorded. This cut ensures both a good quality of event reconstruction and a robust estimation of the exposure of the SD array, which is then obtained in a purely geometrical way. Based on this fiducial cut, any active detector with six active neighbors is defined as a *unitary cell*. From the data set we removed also periods of unstable data acquisition ($\sim 3\%$ of the whole data set), typically associated to the construction phase or due to hardware instabilities.

At the lowest observed energies, around 3×10^{17} eV, the angular resolution of events is contained within 2.2°, which is quite sufficient to perform searches for large-scale patterns in arrival directions, and reaches 1° for events with energy greater than 10^{19} eV.

3. Analysis methods

The Pierre Auger array operates almost uniformly with respect to sidereal time thanks to the Earth's rotation: the zenith angle dependent shower detection and reconstruction are not functions of right ascension but are strong functions of declination. Thus, the most commonly used technique, the *Rayleigh formalism* (originally proposed in Ref. [11]), is the analysis in right ascension only, through harmonic analysis of the counting rate within the declination band defined by the detector field of view. Conventionally, one extracts the first harmonic by measuring the counting rate as a function of the local sidereal time (or right ascension) and fitting the result to a sine wave. The amplitude of the harmonic and the corresponding phase (right ascension of the maximum intensity) are then derived.

The experimental study of large scale CR anisotropies is however challenging since there are several experimental effects (e.g. variations of the detector array area, instabilities and dead times of the apparatus, atmospheric effects) that could bias the measure. A dipolar modulation of experimental origin in the distribution of arrival times of the events with a period equal to one solar day may in fact induce a spurious anisotropy in the right ascension distribution. To identify genuine modulations in the cosmic rays flux it is therefore important to take into account and possibly subtract all the experimental effects. We thus performed two different and complementary analyses: the *Rayleigh analysis weighted by exposure* and the *East–West differential method*.

3.1. Rayleigh analysis weighted by exposure

The relative variation of the integrated number of unitary cells, $\Delta N_{cell}(t) = N_{cell}(t)/\langle N_{cell}(t)\rangle$, is shown in Fig. 1 as a function of solar (*left panel*) and sidereal time (*right panel*). A clear diurnal variation in the exposure is apparent on the solar time scale, showing an almost dipolar modulation with an amplitude of 2.5%. This is due to both the working times of the construction phase of the detector and to the outage of some batteries of the surface detector stations during nights. When averaged over six full years, this modulation is almost totally smoothed out on the sidereal time scale, but it should be taken into account in any case because the amplitude of the sideband effect is proportional to the solar amplitude and can alter the result.

To avoid biases from such spurious modulations in the measure of large scale anisotropies we adopted the classical Rayleigh formalism, slightly modified to account for the non-uniform exposure to different parts of the sky by weighting each event with right ascension α_i with the inverse of the integrated number of unitary cells at the local sidereal time of the event. The Fourier coefficients a and b are calculated as

$$a = \frac{2}{\Omega}\sum_{i=1}^{N}\omega_i \cos\alpha_i, \quad b = \frac{2}{\Omega}\sum_{i=1}^{N}\omega_i \sin\alpha_i \tag{1}$$

where the sum runs over the number of events N in the considered energy range, the weights are given by $\omega_i = [\Delta N_{cell}(\alpha_i^0)]^{-1}$ (α_i^0 is the local sidereal time expressed in radians and chosen so that it is always equal to the right ascension of the

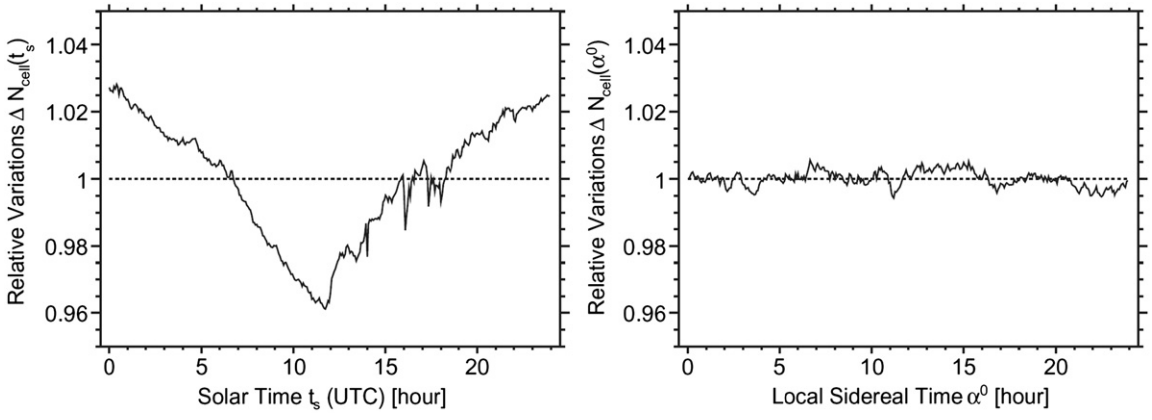

Fig. 1. Relative variation of the integrated number of unitary cells as a function of the solar hour of the day in UTC (*left panel*), and as a function of the local sidereal time (*right panel*).

zenith at the center of the array) and the normalization factor is $\Omega = \sum_{i=1}^{N} \omega_i$. The amplitude r and phase φ are then given by $r = \sqrt{a^2 + b^2}$ and $\varphi = \arctan(b/a)$, and follow respectively a Rayleigh and uniform distributions in the case of an underlying isotropy.

Besides the non-uniform exposure, another bias in the measure of large scale anisotropies can be due to changes in the air density and pressure that affect the development of EAS and consequently the estimation of the energy of each event [12]. To remove these variations the conversion of the shower size into energy is performed by relating the observed shower size to the one that would have been measured at reference atmospheric conditions. Above 1 EeV this procedure allows the size of the sideband amplitude to be reduced to less than 10^{-3}. Below such energy threshold weather effects start to affect also the detection efficiency, as a consequence spurious variations of the counting rate strongly increase and cannot be neglected any more. This analysis method can thus be safely applied only above 1 EeV.

3.2. East-West method

Below 1 EeV we adopt another technique, the differential East–West method [13], based on the analysis of the difference of the counting rates in the East and West directions.

This method relies on the fact that the difference between the observed counting rates of events recorded at each local sidereal time t, arriving from the Eastern and the Western hemispheres, $I_E^{obs}(t)$ and $I_W^{obs}(t)$ respectively, is proportional to the derivative of the true total intensity of cosmic rays $I_{tot}(t)$, the coefficient of proportionality being approximately the mean hour angle $\langle h \rangle$ of the observed events:

$$I_E^{obs}(t) - I_W^{obs}(t) \simeq \langle h \rangle \frac{dI_{tot}^{true}(t)}{dt}. \quad (2)$$

Since the experimental instabilities simultaneously affect both the East and the West sectors (*i.e.* the instantaneous exposure of the two sectors is identical), all the effects of experimental origin, being independent of the incoming direction, are expected to be removed at first order through the subtraction. The method therefore does not require any corrections, thus preventing the possible associated systematics to affect the results, though at the cost of a reduced sensitivity with respect to the standard Rayleigh analysis.

The amplitude r and phase φ of the first harmonic can be calculated from the arrival times of N events using the standard first harmonic analysis slightly modified to account for the subtraction of the Western sector to the Eastern one. The Fourier coefficients a_{EW} and b_{EW} are thus defined by

$$a_{EW} = \frac{2}{N} \sum_{i=1}^{N} \cos(\alpha_i^0 + \zeta_i), \quad (3)$$

$$b_{EW} = \frac{2}{N} \sum_{i=1}^{N} \sin(\alpha_i^0 + \zeta_i),$$

where ζ_i equals 0 if the event is coming from the East or π if coming from the West (so effectively subtracting the events from the West direction). This allows us to recover the right ascension amplitude r and the phase φ_{EW} from $r = (\pi \langle \cos\delta \rangle / 2 \langle \sin\theta \rangle) \sqrt{a_{EW}^2 + b_{EW}^2}$ and $\varphi_{EW} = \arctan(b_{EW}/a_{EW})$, where δ is the declination and θ the zenith angle of the detected events (see Ref. [13] for more details). Note however that φ_{EW}, being the phase corresponding to the maximum in the differential of the East and West fluxes, is related to φ through $\varphi = \varphi_{EW} + \pi/2$.

4. Results

The two analyses have been applied in two different energy ranges: the East–West method below 1 EeV and the Rayleigh analysis above such energy threshold. The amplitude r and the phase φ of the first harmonic resulting from the two analyses are shown in Fig. 2 as a function of energy.

Below 8 EeV the size of the energy intervals is $\Delta \log_{10}(E) = 0.3$, so that it is larger than the energy resolution (about 15% [14]). Above 8 EeV, to guarantee the determination of the amplitude measurement within an uncertainty of $\simeq 2\%$, all events ($\simeq 5000$) are gathered in a single energy interval. In the upper plot of Fig. 2 the dashed line indicates the 99% *C.L.* upper bounds on the amplitudes that could result from fluctuations of an isotropic distribution. There is no evidence of any significant signal in any energy range. The probability with which the 6 observed amplitudes could have arisen from an underlying isotropic distribution is $\simeq 9\%$.

The phase of the first harmonic is shown in the lower plot of the same figure. In this case a smooth transition from a common phase of 270° below 1 EeV to another phase of $\sim 90°$ above 5 EeV is perceptible. This is potentially interesting because the phases are expected to be randomly distributed in case of independent samples whose parent distribution is isotropic. On the contrary, with a real underlying anisotropy, a consistency of the phase

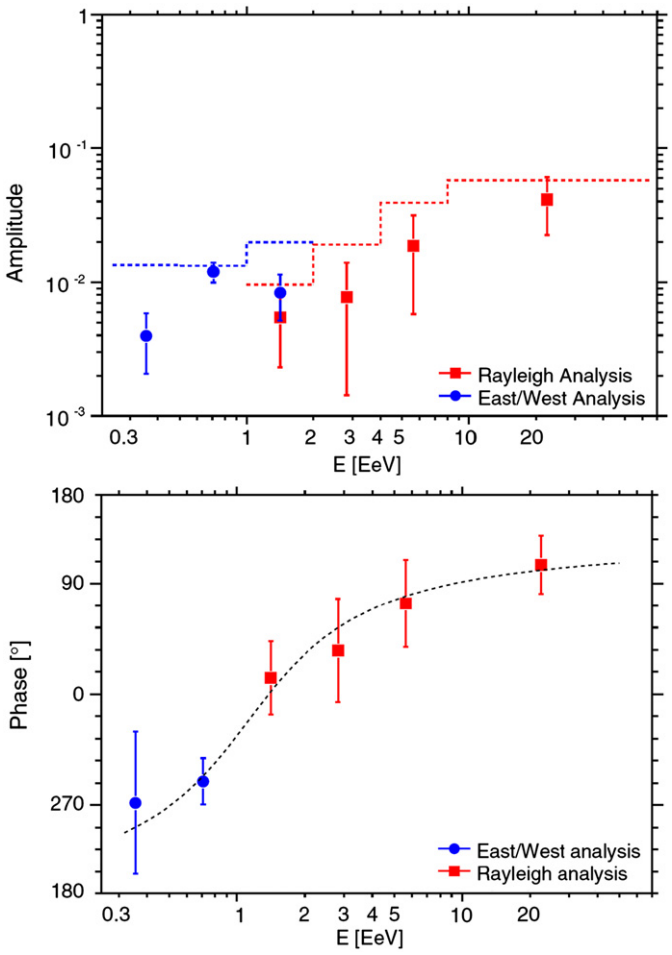

Fig. 2. *Top:* amplitude of the first harmonic as a function of energy. The *dashed line* indicates the 99% *C.L.* upper bound on the amplitudes that could result from fluctuations of an isotropic distribution. *Bottom:* Phase of the first harmonic as a function of energy. The *dashed line*, resulting from an empirical fit, is used in the likelihood ratio test (see text).

measurements in ordered energy intervals is indeed expected to be revealed with a smaller number of events than that needed to detect the amplitude with high statistical significance [15]. Below 1 EeV, besides being constant, the phase is also compatible with the right ascension of the Galactic Center ($\alpha_{GC} = 266.4^{\circ}$) and then moves towards another value. Such transition is an important clue in the study of the transition from galactic to extragalactic origin of cosmic rays.

To quantify whether or not a parent random distribution of arrival directions reproduces the phase measurements in adjacent energy intervals better than an alternative dipolar parent distribution, we use a likelihood ratio test [16]. When applied to the data points of the lower plot of Fig. 2, this test leads to a probability of $\sim 2 \times 10^{-3}$ to accept the random distribution compared to the alternative one. Since we did not perform an *a priori* search for a smooth transition in the phase measurements, we cannot derive a confidence level from this result. To confirm the detection of a real transition at 99% *C.L.* with an efficiency of $\simeq 90\%$ we should repeat the analysis on an independent data set and we need to collect $\simeq 1.8$ times the number of events analysed here.

Results of the first harmonic analysis performed in terms of energy thresholds (strongly correlated bins) are shown in Fig. 3. They provide no further evidence in favor of a significant anisotropy.

To check if the corrections implemented for the Rayleigh analysis take into account all the spurious effects we performed a third complementary analysis: the *Fourier time analysis* [17]. It has been designed to disentangle any sidereal modulation from the solar and the anti-sidereal ones [18] without the knowledge of the exposure. For each frequency we calculate the Fourier transform of the distribution of the times t_i of the events:

$$\tilde{\alpha}_i^0 = \frac{2\pi}{T_{sid}} t_i + \alpha_i - \alpha_i^0, \tag{4}$$

being T_{sid} the sidereal period.

The amplitude of the Fourier modes is shown in Fig. 4 as a function of frequency (the dashed vertical lines represent, from left to right, the anti-sidereal, solar and sidereal frequencies) when considering all the events above 1 EeV. Without implementing any corrections we obtain the blue dotted curve: a net solar amplitude of 3.7% is clearly visible and highly significant. The impact of the correction on the energy estimation is evidenced by the red dashed curve within the resolved solar peak (reduction of 20% of the spurious modulations). Then, accounting also for the exposure variation, the solar peak is reduced at a level close to the statistical noise, as shown by the black thick curve. This evidences that the variations in the exposure and weather effects are under control and are correctly subtracted.

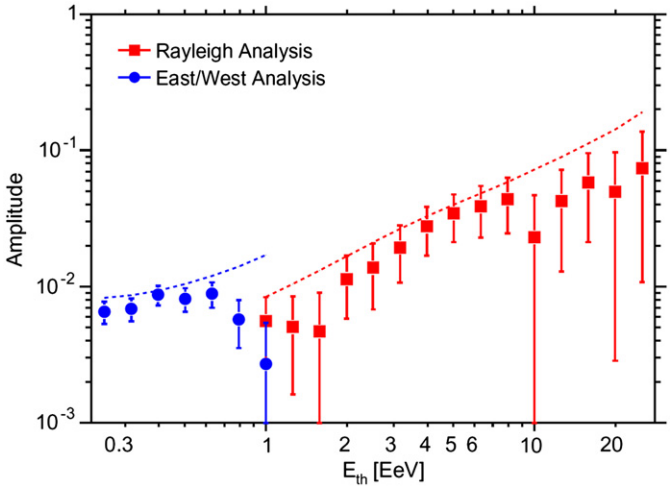

Fig. 3. Amplitude of the first harmonic, as Fig. 2 (*top*), but as a function of energy thresholds.

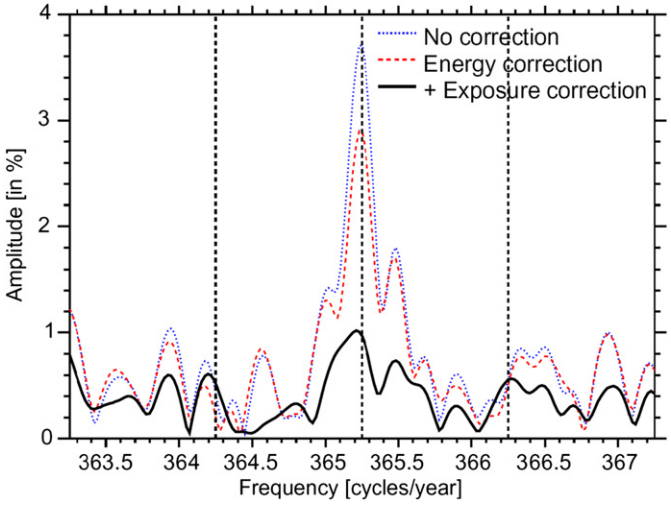

Fig. 4. Amplitude of the Fourier modes as a function of the frequency above 1 EeV. *Blue dotted curve*, before correction of energies and exposure; *red dashed curve*, after correction of energies; *black thick curve*, after correction of energies and exposure; *dashed vertical lines* from left to right, anti-sidereal, solar and sidereal frequencies. (For interpretation of the references to color in this figure legend, the reader is referred to the web version of this article.)

5. Upper limits and comparison with theoretical expectations

Since no significant departure from isotropy is observed and having proved that systematic effects are correctly taken into account, upper limits at 99% *C.L.* can thus be derived using only the statistical uncertainties. Such upper limits are calculated according to the distribution drawn from a population characterised by an anisotropy of unknown amplitude, as derived by Linsley in his 3rd alternative in Ref. [11].

The Rayleigh amplitude measured by an Observatory depends on its latitude and on the considered range of zenith angles. It can be related to real equatorial dipole components $d_{\perp}$ by $d_{\perp} \simeq r/\langle \cos\delta \rangle$ [19], where δ is the declination of the detected events, allowing a direct comparison of results from different experiments and from model predictions. The upper limits on $d_{\perp}$ obtained with this analysis are shown in Fig. 5, together with previous results from EAS-TOP [20], KASCADE [21], KASCADE-Grande [22] and AGASA [6]. The 4% anisotropy reported by AGASA in the 1–2 EeV energy bin is not confirmed by our results (even if a proper comparison should take into account the peculiarities of the two experiments).

In the same figure some predictions for the anisotropies arising from models of both galactic and extragalactic cosmic ray origin are also shown. If the origin at EeV energies is galactic a modulation at the percent level is conceivable. The exact value strongly depends on specific models, three possible scenarios are here presented: *A*, *S* and *Gal*. In models *A* and *S* (*i.e.* Antisymmetric and Symmetric galactic magnetic field), the anisotropy is caused by drift motions due to the regular component of the galactic magnetic field [23], while in model *Gal*, the anisotropy is caused by purely diffusive motions due to the turbulent component of the field [24]. Our current upper limits already exclude predictions from model *A*, put some constraints on model *Gal* and start to become sensitive to the amplitudes predicted by model *S*.

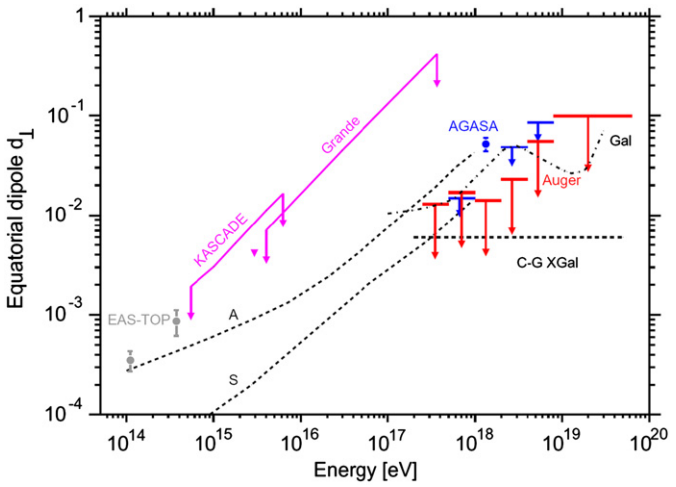

Fig. 5. Upper limits on the anisotropy amplitude of first harmonic as a function of energy from this analysis. Results from EAS-TOP, AGASA, KASCADE and KASCADE-Grande experiments are displayed too, together with expectations from the mentioned theoretical models.

On the other hand, if cosmic rays are dominantly extragalactic at 10^{18} eV, the motion of our galaxy with respect to the CMB (supposed to be the frame of extragalactic isotropy) should induce a small dipolar anisotropy of $\sim 0.6\%$, as predicted by model *C-G Xgal* [25]. The upper limits set in this analysis are getting very close to this amplitude (the statistics required to detect such amplitude at 99% *C.L.* is $\simeq 3$ times the present one).

6. Conclusions

We have searched for cosmic ray large scale anisotropies above 2.5×10^{17} eV with data recorded at the Pierre Auger Observatory by adopting two complementary analyses. Both methods account for the non-uniformity in the acceptance and the weather effect systematics, thus erasing any spurious modulation.

No significant large-scale pattern has been observed, 99% *C.L.* upper limits at the percent level have been set at EeV energies, constraining some theoretical models. The anisotropy reported by AGASA (4% in the 1–2 EeV energy bin) is not confirmed.

In future analyses, we will benefit from the lower energy threshold now available at the Pierre Auger Observatory thanks to the infill array [26]. Preliminary results from the analyses of these data with the East–West method are consistent with the results presented here and, in particular, they show an apparent constancy of the phase below 1 EeV.

References

[1] M. Hillas, Journal of Physics G R95 (2005) J31.
[2] J. Linsley, 8th ICRC Jaipur 4 (1963) 77.
[3] The Pierre Auger Collaboration, Physics Letters B 685 (2010) 239.
[4] V. Berezinsky, Physical Review D 74 (2006) 043005.
[5] D. Allard, et al., Astroparticle Physics 27 (2007) 61.
[6] N. Hayashida, et al., Astroparticle Physics 10 (1999) 303.
[7] D.J. Bird, et al., Fly's Eye Collaboration, Astrophysics Journal 511 (1999) 739.
[8] J.A. Bellido, et al., SUGAR Collaboration, Astroparticle Physics 15 (2001) 167.
[9] The Pierre Auger Collaboration, Astroparticle Physics 27 (2007) 244.
[10] The Pierre Auger Collaboration, Nuclear Instrumentation and Methods in Physics Research A523 (2004) 50.
[11] J. Linsley, Physical Review Letters 34 (1975) 1530.
[12] The Pierre Auger Collaboration, Astroparticle Physics 32 (2009) 89.
[13] R. Bonino, et al., Astrophysics Journal 738 (2011) 67.
[14] R. Pesce, for the Pierre Auger Collaboration, in: Proceedings of 32nd ICRC, Beijing, China, 2011, arXiv:1107.4809[astro-ph.HE].
[15] J. Linsley, A.A. Watson, private communications.
[16] The Pierre Auger Collaboration, Astroparticle Physics 34 (2011) 627.
[17] P. Billoir, A. Letessier-Selvon, Astroparticle Physics 29 (2008) 14.
[18] F.J.M. Farley, J.R. Storey, Proceedings of the Physical Society A 67 (1954) 996.
[19] J. Aublin, E. Parizot, Astronomy & Astrophysics 441 (2005) 407.
[20] The EAS-TOP Collaboration, Astrophysical Journal Letters 692 (2009) 130.
[21] The KASCADE Collaboration, Astrophysical Journal 604 (2004) 687.
[22] S. Over, et al., in: Proceedings of the 30th ICRC, vol. 4, 2007, p. 223.
[23] J. Candia, S. Mollerach, E. Roulet, Journal of Cosmology and Astroparticle Physics 0305 (2003) 003.
[24] A. Calvez, A. Kusenko, S. Nagataki, Physical Review Letters 105 (2010) 091101.
[25] M. Kachelriess, P. Serpico, Physics Letters B 640 (2006) 225.
[26] M. Platino for the Auger Collaboration, in: Proceedings of the 31st ICRC, 2009, arXiv:0906.2354[astro-ph].